

BL28XU (RISING II)

Next-generation vehicles such as electric vehicles and plug-in hybrid vehicles are key technologies to reduce carbon dioxide emissions. The spread of these next-generation vehicles largely depends on the performance and safety of storage batteries. Therefore, the development of a post-lithium-ion battery (LIB) with an energy density far greater than that of the current LIB while maintaining the durability and life equivalency attracts much attention. Currently, Kyoto University has proposed four innovative storage battery systems: nano-interface controlled batteries (halide shuttle batteries and conversion-type batteries), sulfide batteries, and zinc-air batteries, in the Research and Development Initiative for Scientific Innovation of New Generation Batteries (RISING) project. At the same time, various advanced analysis tools have been developed at BL28XU^[1] which is dedicated to the research of innovative storage batteries.

BL28XU mainly develops technology for *in situ* observations of the reaction inside storage batteries via the energy-dispersive confocal diffraction technique^[2, 3], X-ray diffraction spectroscopy analysis^[4-6], hard X-ray photoelectron spectroscopy^[7], etc. Since 2016, the RISING2 project has been ongoing as a contract research project of the New Energy and Industrial Technology Development Organization (NEDO) and is promoting technology development for practical uses of storage batteries. Based on the results of RISING, specific research focuses on three subjects for storage batteries on a wide spatiotemporal scale: (1) elucidation of reaction distribution generation factors, (2) analysis of active material reactions and non-equilibrium

behaviors, and (3) elucidation of electrode/electrolyte interface phenomena. Our goal is to solve these subjects by developing technologies with sufficient spatial and time resolutions. In addition, the technologies to address the following subjects have been developed in the RISING2 project: (4) elucidation of the formation mechanism of random materials such as electrolytic solution and electrolytes at the electrode interface, and (5) elucidation of thermodynamic or physical instability phenomena inside the storage batteries. Here we report representative achievements in FY2018.

1. Confocal X-ray diffraction technique using a two-dimensional detector with a sight-selecting slit

To achieve a longer range, the battery volume must be increased. Large batteries tend to deteriorate due to a non-uniform current distribution inside the composite electrodes. Therefore, we developed a new non-destructive analysis method to evaluate the distribution of active material states using X-ray diffraction (XRD). Because automotive batteries are charged and discharged at a high rate, the analyzing technology should have a high time resolution. Two-dimensional detectors are frequently used for time-resolved X-ray diffraction due to their ability to acquire diffraction figures in one exposure, which is typically completed in only a few seconds.

In the case of automotive batteries employing thick electrodes, the diffraction figure is blurred because multiple diffraction points occur on the incident X-

ray axis. To realize confocal measurements for thick samples, we introduced a sight-selecting slit, which is a single straight slit located between the sample and the two-dimensional detector. The slit edge is declined to the horizontal line by 45° . The slit limits the reach of the diffracted X-ray from the limited area to a specific line on the two-dimensional detector. In the process of converting two-dimensional figures to a one-dimensional diffraction pattern, only data on the specific line are used to extract the confocal XRD profile [8].

Figure 1 shows a schematic drawing of the experimental alignment. Automotive cell (~ 5 Ah capacity) is situated on the sample stage of the diffractometer. The two-dimensional detector, Pilatus 3X CdTe 300 KW, is attached to the 2θ arm of the diffractometer. The camera length is 834 mm. A sight-selecting slit (0.2-mm height) is attached to the 2θ arm, where the distance between the diffraction center and the sight-selecting slit is 275 mm. The energy and size of the monochromatic X-rays are 43 keV and 0.5 mm (horizontal) \times 0.2 mm (vertical). The typical exposure time is set to 5 s. A

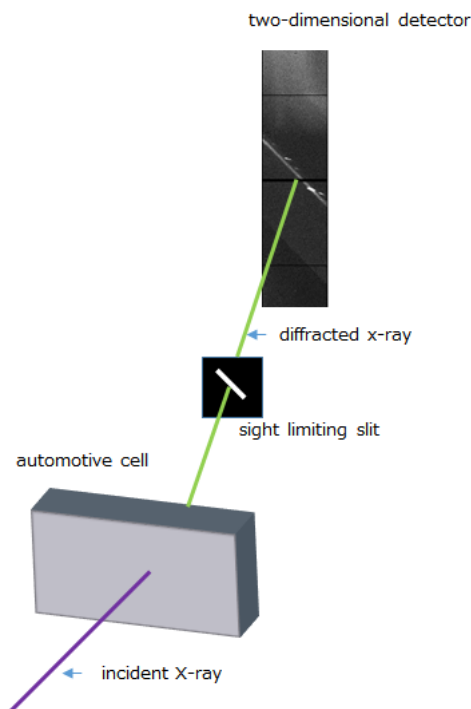


Fig. 1. Schematic of the experimental arrangement.

charge-discharge device is connected to the cell to perform an *operando* experiment.

Figures 2(a) and 2(b) show the time-resolved XRD patterns of the positive electrode region during 1 C charge-discharge of an automobile cell for the upstream ($y = -5$ mm) and downstream ($y = 5$ mm)

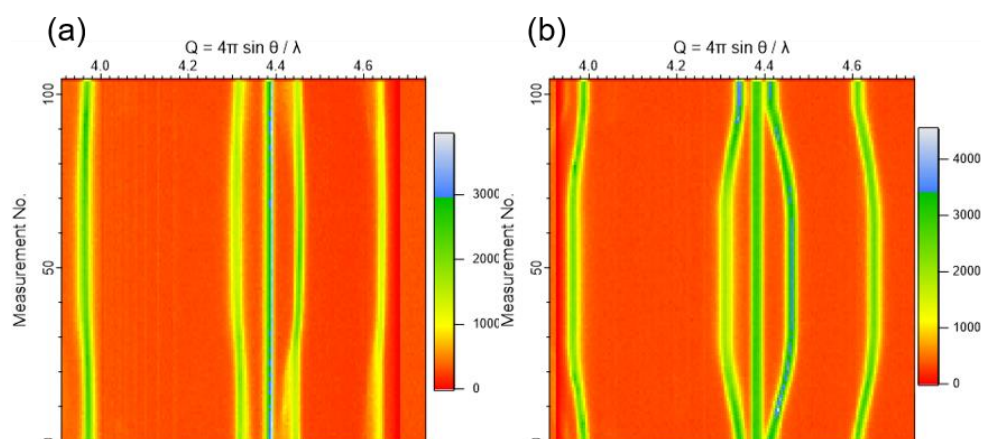


Fig. 2. Time-resolved XRD pattern of the cathode region during 1 C charge discharge of an automobile cell for (a) the upstream ($y = -5$ mm) and (b) downstream ($y = 5$ mm) positions.

positions. The origin of the y -coordinate is the center of the diffractometer. Although the measurement was performed once, the acquired diffraction figures contained space-resolved information along the X -rays, which is easily extracted by an analyzing program. The peak shift of the cathode in the upstream position was much smaller than that in the downstream position. In the same experiment, the XRD pattern of the negative electrode region was measured by flipping the 2θ angle and the z -coordinate of the sight-selecting slit after each exposure.

2. Development of imaging-XAS using a K-B mirror system

New large-capacity electrode materials based on a conversion reaction are investigated as a post-lithium-ion battery. One typical conversion reaction is $\text{FeF}_3 + 3\text{Li} \rightarrow \text{Fe} + 3\text{LiF}$ or $\text{Fe}_2\text{O}_3 + 6\text{Li} \rightarrow 2\text{Fe} + 3\text{Li}_2\text{O}$ during the discharge process. In the former case, FeF_3 and Li serve as the positive and negative electrodes, respectively. The battery operates by the transfer of lithium ions between the positive and negative electrodes. Non-uniformity in the lithium-ion transfer results in insufficient performance and stability. Therefore, X-ray absorption spectroscopy (XAS) with a two-dimensional detector, imaging-XAS, was used to visualize the lithium-ion-reaction distributions within the battery cell. Since valence changes compensate for the charge valence in the positive electrode during the transfer of lithium ions, imaging-XAS can show valence images of transition metals in the electrode that are equivalent to the lithium-ion-reaction distributions.

Since the beam-size of 0.5-mm square in undulator beamlines is too small to visualize the reaction distributions, the X-ray beam was magnified by a

Kirkpatrick-Baez (K-B) mirror system. The X-ray beam size and flux can be changed at the measurement points from the focal point of the K-B mirror. The beam-size was $1.3 \mu\text{m} \times 3 \mu\text{m}$ at the focal point and $1 \times 2 \text{mm}$ at the measurement point, which was 400 mm away from the focal point.

The battery cells were fabricated by Fe_2O_3 , lithium-foil, and an electrolyte-soaked polypropylene separator with an aluminum-laminated film. The *operando* imaging XAS spectra of the cell at the Fe K-edge by a transmission mode were measured during the discharge-charge process at current rate of 0.2 C between 0.05 V and 3 V. While the X-ray energy was scanned from 7100 eV to 7150 eV by a channel cut monochromator [Si(111)], the imaging-XAS spectra were measured using the two-dimensional detector system composed of a P43 scintillator, optical lens, and a CCD array detector (C9100; Hamamatsu Photonics) with an effective pixel size of $6.5 \mu\text{m} \times 6.5 \mu\text{m}$ by a two-times optical magnification.

The exposure time per image and X-ray energy step were 1 s and 0.5 eV, respectively. The spatial resolution of the detector system, which was confirmed by observations of a standard patterned specimen, was 10 μm . The high X-ray flux at the undulator beamline allows imaging-XAS spectra of the two cells to be measured in turns (one cycle of 517 s). The results of the imaging-XAS measurement show that areas of FeO_x and Fe are separated at the final discharge process and correspond to the conversion reaction.

Acknowledgments:

This work was supported by NEDO under the RISING2 project.

Kenji Sato^{*1}, Tastumi Hirano^{*2} and Hisao Kiuchi^{*2}

^{*1} Honda R&D Co., Ltd.

^{*2} Office of Society-Academia Collaboration for
Innovation, Kyoto University

Reference:

- [1] H. Tanida et al., *J. Synchrotron Radiat.* **21**, 268 (2014).
- [2] H. Murayama et al., *J. Phys. Chem. C* **118**, 20750 (2014).
- [3] H. Murayama et al., *Journal of JSSRR* **28**, 161 (2015).
- [4] T. Kawaguchi et al., *J. Synchrotron Radiat.* **21**, 1247 (2014).
- [5] T. Kawaguchi et al., *Phys. Chem. Chem. Phys.* **17**, 14064 (2015).
- [6] T. Kawaguchi et al., *Journal of JSSRR* **28**, 124 (2015).
- [7] K. Shimoda et al., *J. Mater. Chem. A* **4**, 5909 (2016).
- [8] Japan Patent 6383018 (granted 2018)